Doctoral Degree Under Co-Tutoring Agreement Between

Czech Technical University in Prague

and

Universitat Politècnica de Catalunya

THESIS STATEMENT

Vojtěch Bělohlav

2021

CZECH TECHNICAL UNIVERSITY IN PRAGUE

FACULTY OF MECHANICAL ENGINEERING

DEPARTMENT OF PROCESS ENGINEERING

THESIS STATEMENT

Intensification of mixing and homogenisation of culture medium in photobioreactors for microalgae production

Vojtěch Bělohlav

Doctoral study programme: Mechanical Engineering

Field of study: Design and Process Engineering

Supervisors: prof. Ing. Tomáš Jirout, Enrica Uggetti

Dissertation thesis statement for obtaining the academic title of „Doctor“ abbreviated as „PhD“

Prague July, 2021

Title in Czech language: Intenzifikace míchání a homogenizace kultivačního média ve fotobioreaktorech pro kultivaci mikrořas

This thesis is an outcome of a full-time doctoral study programme at the Department of Process Engineering, Faculty of Mechanical Engineering, Czech Technical University in Prague (CTU) and Department of Civil and Environmental Engineering, Universitat Politècnica de Catalunya.

Author: Ing. Mgr. Vojtěch Bělohlav

Department of Process Engineering, Faculty of Mechanical Engineering, CTU

Technická 4, Prague, 160 00, Czech Republic

Supervisor: prof. Ing. Tomáš Jirout, PhD

Department of Process Engineering, Faculty of Mechanical Engineering, CTU

Technická 4, Prague, 160 00, Czech Republic

Supervisor: Enrica Uggetti

Department of Civil and Environmental Engineering, Universitat Politècnica de Catalunya

Jordi Girona 1-3, Barcelona, 08034, Spain

Co-supervisor: doc. Ing. Lukáš Krátký, PhD

Department of Process Engineering, Faculty of Mechanical Engineering, CTU

Technická 4, Prague, 160 00, Czech Republic

Reviewers:

Ricardo Blanco Aguilera

Roman Fekete

Radek Šulc

The thesis statement was sent out on: .....

The defence of the thesis will take place on .....

The thesis is available on the Department of Process Engineering, Faculty of Mechanical Engineering, CTU, Technická 4, Prague.

Tomáš Jirout

Head of Doctoral Study Field Design and Process Engineering

Faculty of Mechanical Engineering, CTU

List of contents

1 Introduction

Microalgae biomass is classified as a third-generation feedstock and has a potential for biofuel, food, feed and chemical production. The characteristic of microalgae is that they are able to convert sunlight, CO_2, and nutrients into biomass through photosynthesis in the same way as other plants. However, microalgae have higher photosynthetic efficiency than other crops, which leads to a higher conversion of CO_2 to microalgae biomass. They can grow at a faster rate than other land-based crops and can live in a diverse environment with basic nutrient requirements (Milano et al., 2016).

2 State of the art

In order to reach a full industrial scale for microalgal biomass processing technologies and for final products to be competitive on the market, it is necessary to increase the efficiency of the cultivation process itself and to optimize the systems for microalgae cultivation.

2.1 Operating parameters to be considered for scale-up

Proper microalgae growth and biomass productivity depend on several operational and design factors. Generally, microalgae need light, nutrients, a carbon source, and a certain temperature to grow properly (Masojídek, 2014).

2.2 Hydrodynamics influence on microalgae cultivation

As the hydrodynamics of the culture medium is very important for streamlining the process of microalgae cultivation in PBRs, an overview of studies aimed at modeling and investigation of the influence of hydrodynamic conditions on microalgae cultivation is presented in the thesis.

2.2.1 Microalgae models

A number of different models have been developed to describe the photosynthesis and process of microalgae cultivation, which can be specified in terms of biomass growth, nutrients utilization, or the influence of light, temperature or pH. Solimeno et al. (2017a) created a BIO_ALGAE mechanistic model that describes the complex function of a system for the cultivation of microalgae and bacteria. The BIO_ALGAE model works on the assumption that the culture medium is ideally mixed. The light is thus ideally distributed, and the temperature of the culture medium is homogeneous throughout the volume of the PBR. All these assumptions can be considered for simplification in laboratory systems and pilot PBRs. However, with the transition to a larger scale device, the usability of BIO_ALGAE may be limited. Application of Computational fluid dynamics (CFD) simulations can provide information that would further refine the homogeneity of the concentration of individual components important for the growth of microalgae..

2.2.2 Hydrodynamic conditions in cultivation systems

Mixing affects the mass transfer and subsequently to the utilization of nutrients and carbon dioxide for the growth of microalgae. It is important to ensure that no sedimentation of microalgae cells occurs. It is also necessary to provide homogenous light irradiation of cells in the culture medium. Due to the higher

biomass concentrations or large layer thicknesses of the culture medium, scattering can occur, which can significantly affect the efficiency of the cultivation system (Perner-Nochta and Posten, 2007). This can lead to the formation of dark zones in the culture medium, where the cells do not receive a sufficient amount of light radiation (Zhang et al., 2013).

3 Objectives and thesis outline

The overall objective of the present PhD thesis was to study and optimize the operating conditions of two cultivation systems in order to intensify microalgae production. A hybrid horizontal tubular photobioreactor (HHT PBR) and a closed flat panel photobioreactor (FP PBR) were selected for the study. The majority of existing cultivation systems work efficiently only on a laboratory scale. However, as their design is scaled-up, significant operational problems arise and their applicability on a pilot or industrial scale is limited. Hydrodynamics in cultivation systems has a strong influence during scaling-up, since it affects all parameters important for microalgae cultivation. For this reason, the first objective was to study the hydrodynamic conditions of existing cultivation systems creating a mechanistic model to simulate microalgae cultivation. Experimental measurements were then performed to calibrate and validate the model. Finally, the results of the model were used to optimize the operating conditions and design parameters of the studied PBRs.

3.1 Objectives

The specific objectives of this research were:

- Calibrate a mechanistic model simulating the process of microalgae cultivation in HHT PBR based on the intensive experimental campaigns.
- Calibrate and validate the Computational fluid dynamic (CFD) model simulating hydrodynamic conditions in HHT PBR based on the experimental measurements.
- Integrate the influence of hydrodynamic conditions into a mechanistic model that would consider the influence of hydrodynamics in HHT PBR on the microalgae cultivation process.
- Specify the influence of different operating conditions on the hydrodynamics of the culture medium and the process of microalgae cultivation in HHT PBR.
- Validate the CFD model simulating hydrodynamic conditions in FP PBR based on the experimental measurements.
- Specify the influence of different operating configurations on the hydrodynamics in FP PBR and influence on the formation of biofilm as the key factor affecting the scale-up of cultivation systems.
- Optimize the operating conditions of HHT PBR and FP PBR according to the results of experimental measurements and numerical simulations in terms of the intensification of microalgal biomass production.
- Optimize the design of the FP PBR chamber concerning the intensification of mixing and homogenization of the culture medium. Based on experimental measurements and the created CFD models, verify the usability of internal installations in FP PBR chamber for intensification of mixing and homogenization of culture medium flow.

4 Modeling of hybrid horizontal tubular PBR performance and hydrodynamics

In order to study the influence of hydrodynamic conditions on the cultivation process, it is necessary to create a model that will be able to predict microalgal biomass growth depending on different operating conditions. For this purpose, it is necessary to create a validated hydrodynamic model, which will be able to simulate in detail the local hydrodynamic parameters. The results of the hydrodynamic model can be subsequently integrated into a numerical model that is able to predict microalgal biomass production. For this purpose, the numerical BIO_ALGAE model, which was created at the Universitat Politècnica de Catalunya, can be used. However, before the integration itself, BIO_ALGAE model needs to be validated based on the experimental data from an intensive measurement campaign in hybrid horizontal tubular PBR. Using the integrated model and hydrodynamic model, it is possible to subsequently optimize the operating and design parameters of the PBR.

4.1 Photobioreactor design and system operation

The hybrid horizontal tubular photobioreactor consists of two open retention tanks connected through 16 low-density polyethylene transparent tubes with d=125 mm inner diameter. The total volume of the culture medium in each PBR is 11.7 m^3. The paddle wheel moves the culture medium from one side of the tank over the overflow to the other side. The overflow plate, thus, causes the creation of the difference of culture medium levels Δh (m). The scheme of PBR and section of open retention tank is shown in Figure 4.1.1. The speed of rotation of the paddle wheel determines the level of the culture medium in the suction and discharge section of the paddle wheel, h_2 (m) and h_1 (m) respectively. In the second tank, the medium is moved through the overflow again, thus, continuous circulation in PBR is ensured.

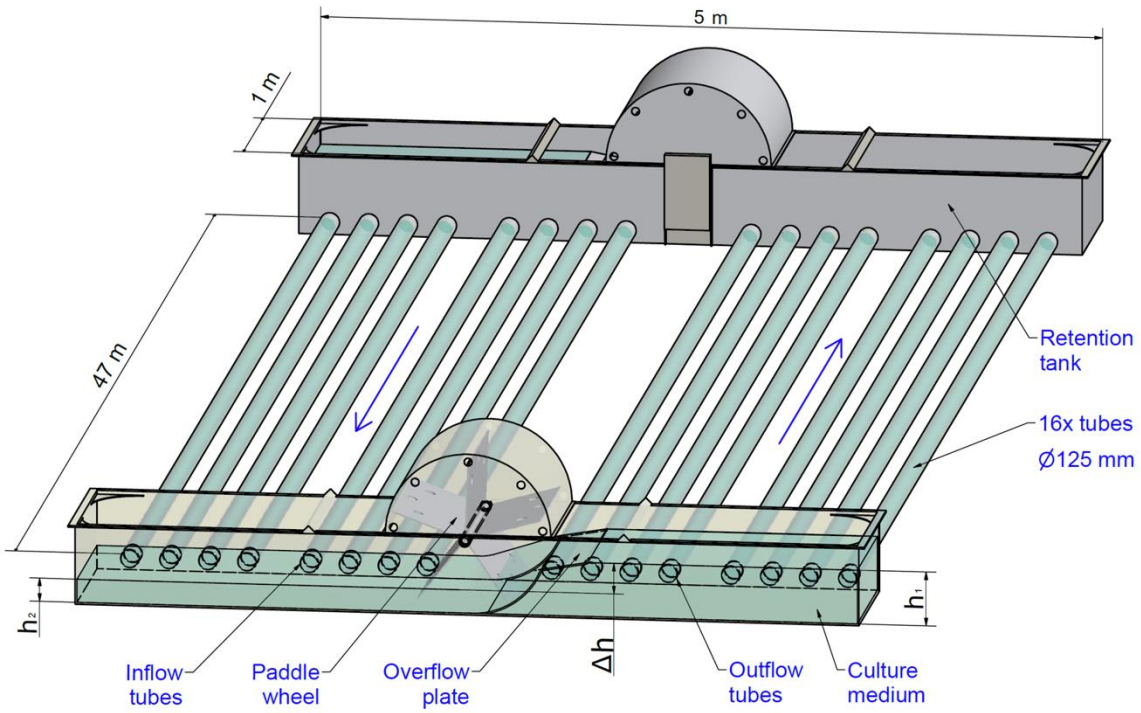

Fig. 4.1.1. 3D isometric view of HHT PBR.

4.2 Calibration and validation of BIO_ALGAE model

The main objective of the present study was to evaluate the daily variations in the performance of HHT PBR for culturing wastewater-borne microalgae, fed with agricultural runoff in different seasons. The results of intensive experimental campaigns can then be used to calibrate and validate the BIO_ALGAE model simulating the microalgae cultivation process.

4.2.1 Monitoring of the PBR performance

Daily changes in the performance were studied in one of HHT PBR during two intensive sampling campaigns carried out in late winter (19th-22nd March 2018) and in mid-spring (8th-11th May 2018). In each campaign, grab samples of the mixed culture medium were collected from one of the two open tanks for three consecutive days every 3 hours, resulting in 8 samples per day. Additionally, one influent sample was collected every sampling day.

4.2.2 Model calibration and validation

The BIO_ALGAE model was implemented in COMSOL Multiphysics™ version 5.4. The model was calibrated and validated using measured data from the winter and spring experimental campaigns. The numerical model was calibrated by comparing the generated graphic data from the model with the measured curves. The following parameters were used for calibration: S_{O2}, *TSS*, and S_{NH4}. The resulting curves of the calibrated model are shown in Figures 4.2.2.1 to 4.2.2.3.

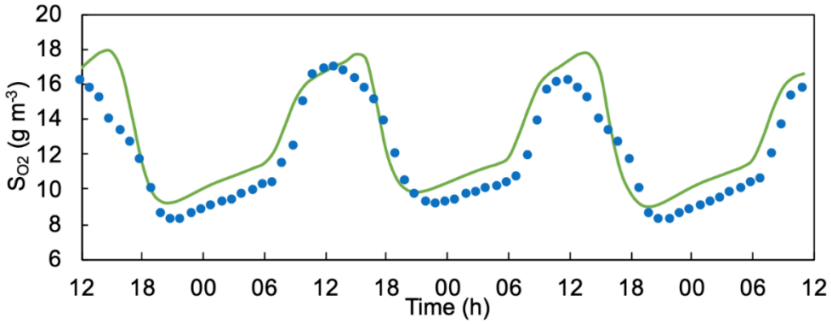

Fig. 4.2.2.1. Calibration of dissolved oxygen in HHT PBR. Simulated (green line) and experimental (blue dots) data during winter measuring campaign.

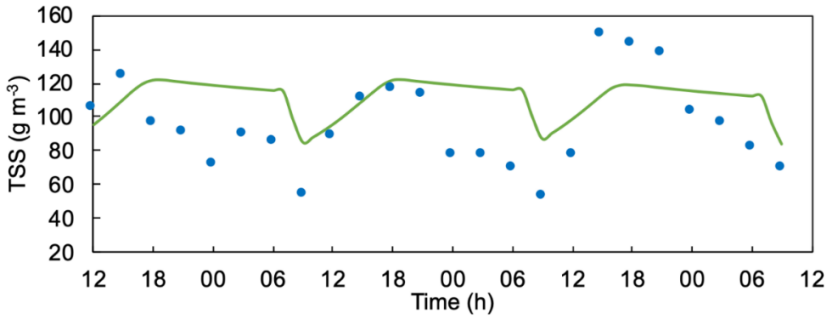

Fig. 4.2.2.2. Calibration of TSS in HHT PBR. Simulated (green line) and experimental (blue dots) data during winter measuring campaign.

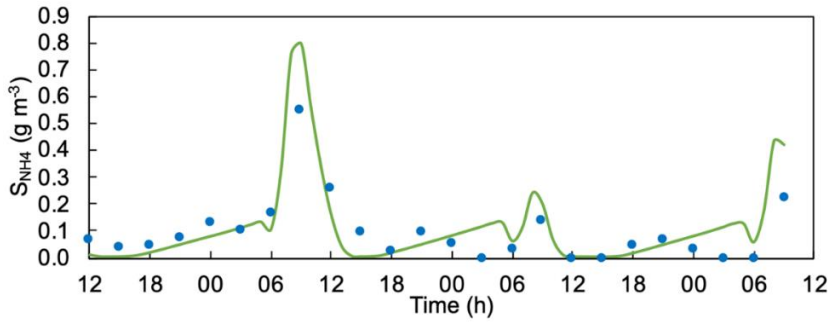

Fig. 4.2.2.3. Calibration of ammonium nitrogen in HHT PBR. Simulated (green line) and experimental (blue dots) data during winter measuring campaign.

Calibration was performed in order to minimize the root mean square error (RMSE). The RMSE of the calibrated model for each component was: $RMSE_{SO2}$ = 1.52 gO_2 m^{-3}, $RMSE_{TSS}$ = 9.48 gTSS m^{-3} and $RMSE_{NH4}$ = 0.05 gNH_4-N m^{-3}. The higher value of $RMSE_{TSS}$ is due to the model considering respiration at the end of the night, resulting in a steep drop in biomass. The decrease in experimentally measured TSS during the night cycle is due to low oxygen production in the culture medium, which keeps the biomass buoyant. The model was validated according to experimental data from the spring campaign. Experimental data matched well with simulated data. The global error of the simulations was slightly higher in comparison with calibration. The RMSE value of each component was: $RMSE_{SO2}$ = 2.43 gO_2 m^{-3}, $RMSE_{TSS}$ = 21.19 gTSS m^{-3} and $RMSE_{NH4}$ = 0.08 gNH_4-N m^{-3}.

4.3 Hydrodynamic conditions in HHT PBR

The aim of this part of the study was to analyze hydrodynamic conditions by CFD simulation in HHT PBR. The numerical model was calibrated and validated on the basis of experimental data, confirming its suitability for simulating the microalgae cultivation process and the need for further investigation.

4.3.1 Hydrodynamic conditions characterization

A set of experimental tracer tests were performed in the tubes of the PBR in order to determine the residence time distribution (RTD). The tests were performed in the tubes, instead of the whole PBR, aimed at estimating the mean residence time and main hydrodynamic characteristics in the irradiated area of the PBR.

Measurement of hydrodynamic characterization

The RTD in the horizontal tubes of the PBR was determined experimentally by the pulse-input tracer technique. The experiments were conducted in 8 tubes under the same operational conditions, i.e. the same rotational speed of the paddle wheels. The tests were performed from the inlet of the tubes in one open tank to the outlet in the other open tank. A concentrated solution of sodium chloride was used as a tracer for the RTD tests. A pulse of the tracer solution was injected by means of a syringe at the inlet of each tube at time zero, and the electrical conductivity was continuously measured and recorded at the outlet of the tubes. Subsequently, measured conductivity values were converted to concentrations. Additionally, two more tracer tests were performed in one tube under different operational conditions,

modifying the difference in the water level in the open tanks. The rotational speed of the paddle wheels was modified in order to set different water levels in the tanks. These tests were used for the preliminary validation of the model. In addition, an ultrasonic flowmeter was installed in order to measure the actual velocity of the culture medium inside the tubes and to verify the accuracy of the pulse input tracer test. The RTD obtained experimentally in the horizontal tubes of the PBR are shown in Figure 4.3.1.1. Experimental tests were performed in the eight tubes, however, results corresponding to Tube 4 are not presented since measurements were not reliable due to a high biofilm concentration on the tube walls. The operating conditions of the PBR (i.e. the rotational speed of the paddle wheels) were set so the culture medium levels h_1 and h_2 in open tanks were 0.28 m and 0.24 m, respectively. The shape of the RTD in all the tubes present a sharp peak, resembling to plug flow with small axial dispersion. All the tubes showed similar behavior, with the peak occurring close to the normalized time θ=1. Note that the normalized time is obtained based on the measured mean residence time t_m (s).

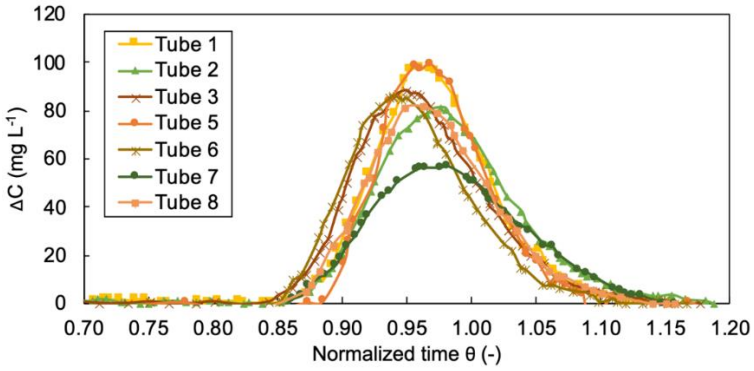

Fig. 4.3.1.1. RTD in the horizontal tubes of the PBR. The difference of concentration is ΔC and θ is the normalized time (dimensionless) $=t_i/t_m$.

The values of mean residence time t_m (s) and the variance are presented in Table 4.3.1.1. Based on the mean residence time t_m (s) and the length of the transparent HHT PBR tube L=47 m, it was possible to determine the mean flow velocity $\bar{u}$ (m s^{-1}) in the tubes and the dimensionless dispersion coefficient D_{ax}. These flow velocities generate a turbulent flow in the tubes, characterized by the Reynolds number ranging from 17,500 to 23,700. The dispersion coefficient can be used to quantify the extent of the axial dispersion in the tubes.

Table 4.3.1.1. Mixing characteristics in horizontal tubular photobioreactor.

Tube Nr.	t_m (s)	$\bar{u}$ (m s^{-1})	u_{max} (m s^{-1})	σ_t^2 (s^2)	σ^2 (-)	D_{diff} (m^2 s^{-1})	D_{ax} (-)
1	250	0.19	0.22	368.6	0.0059	0.0261	0.0029
2	274	0.17	0.20	422.8	0.0056	0.0226	0.0028
3	282	0.17	0.20	541.8	0.0068	0.0267	0.0034
4	N/A	N/A	N/A	N/A	N/A	N/A	N/A
5	254	0.18	0.21	282.5	0.0044	0.0190	0.0022
6	295	0.16	0.19	869.0	0.0100	0.0374	0.0050
7	335	0.14	0.17	954.6	0.0085	0.0280	0.0042
8	288	0.16	0.19	676.5	0.0314	0.0314	0.0041

The difference in hydrodynamic conditions in the PBR tubes was influenced by the formation of biofilm on the inner wall of the tubes due to the organic matter present in the culture medium. Such biofilm can

increase the pressure drop causing constant changes in the flow regime. In order to prevent the formation of biofilm, it is necessary to increase the flow rate velocity of the culture medium and thereby intensify the mixing and the effect of shear forces on the inner wall of the tubes, thus reducing the need for physical cleaning.

4.3.2 Numerical model setup

Two CFD geometries for PBR simulation were created in ANSYS FLUENT CFD 19.1. The 3D geometry was developed to simulate hydrodynamic conditions in open tanks and tubes. The 2D mesh was created only for the detailed description of hydrodynamics in tubes. In order to reduce cells and have still a good resolution, symmetry was anticipated and only half of the PBR tube was simulated in the 2D mesh.

Particle tracking

The particle tracking injection function was used to monitor the movement of microalgal cells in the culture medium during its flow in the tube. The parameters of selected particles were adjusted according to the properties of microalgal cells (Belohlav and Jirout, 2019). The single injection method was chosen for the entry of particles into the tube and the injection point was located at the lower part of the tube at a distance of 0.062 m from the tube axis. The injection point was chosen according to the possibility to simulate the movement of a particle that occurs in the area of the tube that is least irradiated by the light source (dark zone, which is the most unfavorable condition).

A model with a larger diameter of transparent tubes was also created to evaluate the hydrodynamic conditions during the scale-up of the cultivation system. In order to compare the hydrodynamic conditions in geometrically similar tubes to the original HHT PBR, a tube with a diameter of 200 mm was created. In order to make it easier to identify the dimensions, the diameter of the original HHT PBR tubes (125 mm) is marked d_1 (m), and geometrically similar tubes with a diameter of 200 mm are marked d_2 (m). Subsequently, the mesh was created also for tube d_2. Proportionally to tube d_1, the injection point was placed in the least irradiated area of the tube, which corresponds to a distance of 99 mm below the tube axis.

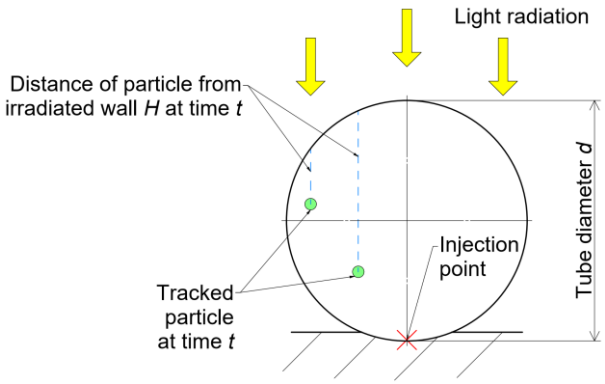

Fig. 4.3.2.1. Scheme of the particle tracking model principle, *H* represents the distance of the particle from the irradiated wall, *d* indicates the tube diameter.

To simulate the intensity of the light radiation received by the microalgae cells from the incident light on the tube walls, it is important to monitor the distance of the cells from the irradiated wall of the tube. The

cell position is thus defined as the vertical distance from the irradiated tube wall *H* (m), since it is assumed that the light source is located directly above the HHT PBR tubes. The scheme of the particle tracking system principle and the marked starting injection point is shown in Figure 4.3.2.1.

4.3.3 Calibration and preliminary validation of CFD model

Figure 4.3.3.1 shows the velocity profile simulated by the CFD model in a cross-section of Tube 1, together with the power-law, the universal smooth tube, and the universal fully rough tube velocity profiles based on the experimental data. The analytical velocity profiles based on experimental data were in good agreement with CFD simulation.

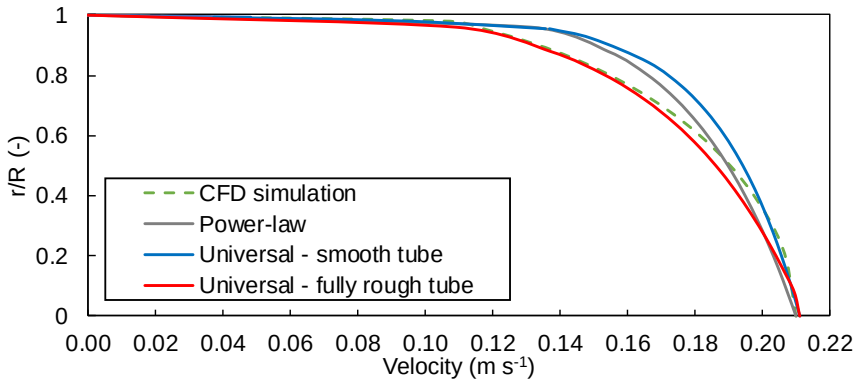

Fig. 4.3.3.1. Comparison of analytical calculation and numerical simulation of velocity profiles inside a tube of the PBR – calibration: Δh=0.04 m, *Re*=23,700; *r* indicates the radial coordinate and R is the inner radius of the tube.

Three different operational configurations were selected to validate the CFD simulation. The water level in the open tanks h_1 (m) and h_2 (m) have been changed by the variation of the paddle wheel rotational speed, resulting in three different configuration setups (A, B, C) as shown in Table 4.3.3.1. For each operational configuration, RTD was determined by the pulse-input tracer measurement done in Tube 1.

Table 4.3.3.1. Operational setup in HHT PBR.

Configuration	h_1 (m)	h_2 (m)	Δh (m)	t_m (s)	$\bar{u}_{tracer}$ (m s^{-1})	$\bar{u}_{flowmeter}$ (m s^{-1})	*Re* (-)
Calibration	0.28	0.24	0.04	247	0.19	N/A	23,700
A	0.35	0.29	0.06	186	0.25	0.249	31,200
B	0.36	0.26	0.10	145	0.32	0.319	39,900
C	0.39	0.26	0.13	128	0.37	0.371	46,200

The velocity profiles inside the tube in the three different conditions were simulated without changing any parameter in the CFD model. The results of the simulations were compared with the universal velocity profiles for rough tubes based on experimental data in Figure 4.3.3.2. CFD simulations were in good agreement with the analytical profiles. Thus, the numerical predictions were preliminarily validated by the experimental data, indicating that the established CFD simulation model can be adapted to simulate the fluid field in the HHT PBR.

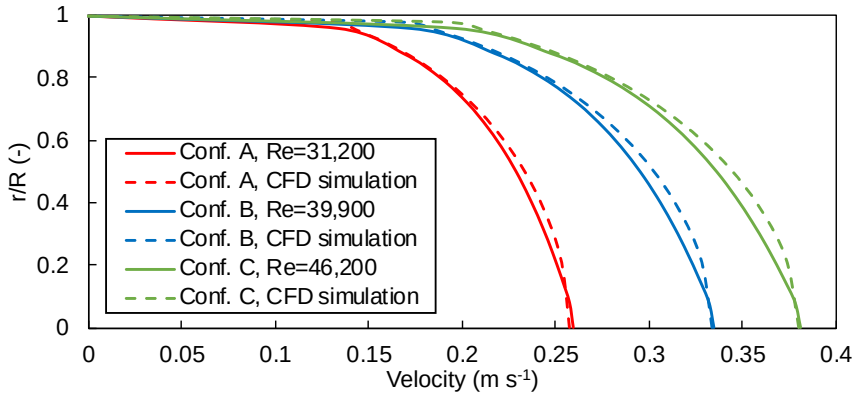

Fig. 4.3.3.2. Preliminary validation of the CFD model: comparison of simulations under the three different conditions considered and the universal velocity profiles for hydraulically rough tubes, *r* indicates the radial coordinate and *R* is the inner radius of the tube.

4.3.4 Simulation of fluid dynamics

Velocity contours

This study was focused on the numerical investigation of overall hydrodynamic conditions in HHT PBR. The hydrodynamics in the open tanks of the PBR was analyzed using the validated 3D model. For small differences in culture medium levels (Δh=0.04 m), low velocities were reached in a significant volume of the tank, in particular in the zone further from the paddle wheels, where the velocity reached values lower than 0.1 m s^{-1}. This low velocity can cause microalgae sedimentation and accumulation in the open tanks (Chisti, 2016). The volume of the open tank consisted of 47 % of the medium flowing with a velocity lower than 0.1 m s^{-1}. The increase in the difference in the water level could reduce the extent of this zone. With a difference of water level Δh of 0.13 m, the velocity in the zone further from the paddle wheels increased, significantly reducing the volume with the low velocity of 23 % of total open tank volume. However, flow velocity was lower than 0.1 m s^{-1} in some specific volumes of the open tank. This suggests that sedimentation and accumulation of microalgae in the tanks cannot be completely avoided by changing the operating conditions. These results also suggest that the shape of the open tanks could be improved in order to further reduce the extent of dead volumes, for instance substituting the corner located opposite to the paddle wheel and tubes with a chamfer or round shape.

Shear stress distribution

The shear force close to the inner wall of the tube is a very important parameter for HHT PBR operation due to its role in avoiding biofilm formation and/or excessive growth. In HHT PBR, the shear stress in the tubes can be increased by increasing the water level difference Δh in the open tanks. The CFD simulation of shear stress distribution for various operational conditions (detailed in Table 4.3.3.1) is shown in Figure 4.3.4.1. The shear stress values on the wall were higher than the critical value of the shear stress at which microalgae is fixed on the transparent walls in closed systems working in controlled laboratory conditions. At values lower than 0.2 Pa, a biofilm layer is formed in a closed cultivation system. However, in order to disrupt the integrity of the already formed biofilm, it is necessary to reach values of shear stress on the wall higher than 6 Pa (Belohlav et al., 2020; Zakova et al., 2019). Therefore, these results suggest that the biofilm could not be removed by the shear forces once it is formed in the

HHT PBR. Physical cleaning of the tubes should be periodically performed. However, the shear force obtained with the highest velocities seems to be able to prevent or reduce the formation of biofilm, thus reducing the need for cleaning or increasing the time interval between consecutive cleanings.

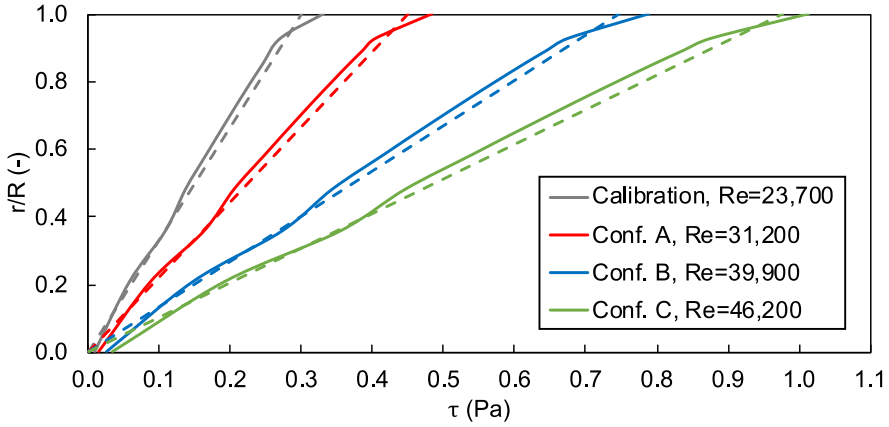

Fig. 4.3.4.1. Total shear stress distribution inside HHT PBR tube, the solid lines represent the distribution from the CFD simulation, the dashed lines represent the distribution determined from the pressure differential, *r* indicates the radial coordinate and *R* is the inner radius of the tube.

4.3.5 Particle tracking

The particle tracking simulation was performed for three operating configurations corresponding to the different rotational speeds of the HHT PBR paddle wheel. Three operating modes were selected to simulate particle tracking, which describes the minimum and maximum operating conditions (calibration and configuration C from Table 4.3.3.1). Configuration A, which corresponds to the flow rate most often used during the cultivation, was included for comparison as well. It is important to provide sufficient solar radiation for all microalgal cells in order the ensure effective cultivation. Therefore, the movement of the particle and its distance from the irradiated surface of the tube was monitored (Figure 4.3.2.1). The distance of the particle from the irradiated wall *H* (m) during the flow through the tube is shown in Figure 4.3.5.1. From the comparison, it can be seen that at lower flow velocities, the particles were still moving close to the initial position. As the flow rate increases, the particles more often get closer to the irradiated area of the tube.

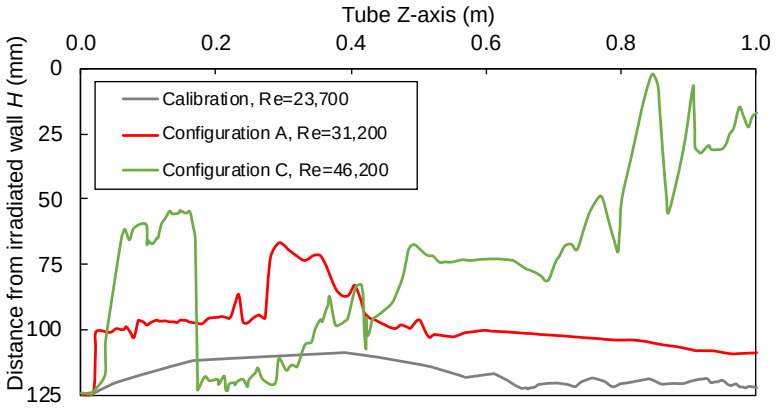

Fig. 4.3.5.1. Distance of the particle from irradiated wall in HHT PBR tube.

To compare the distances of the cells from the irradiated wall for geometrically similar tubes, the depth was related to the diameter of the tubes *d* (m). The dimensionless distance from the irradiated wall *H/d* is shown in Figure 4.3.5.2. A mean value of the dimensionless distance from the irradiated wall (dashed line) was generated for each configuration as well. It can be seen from the comparison that the dimensionless distance from the irradiated wall was comparable for geometrically similar tubes at the same flow regime. The hydrodynamic conditions based on the original CFD model for the tubes d_1 are therefore also applicable to geometrically similar systems with a different scale.

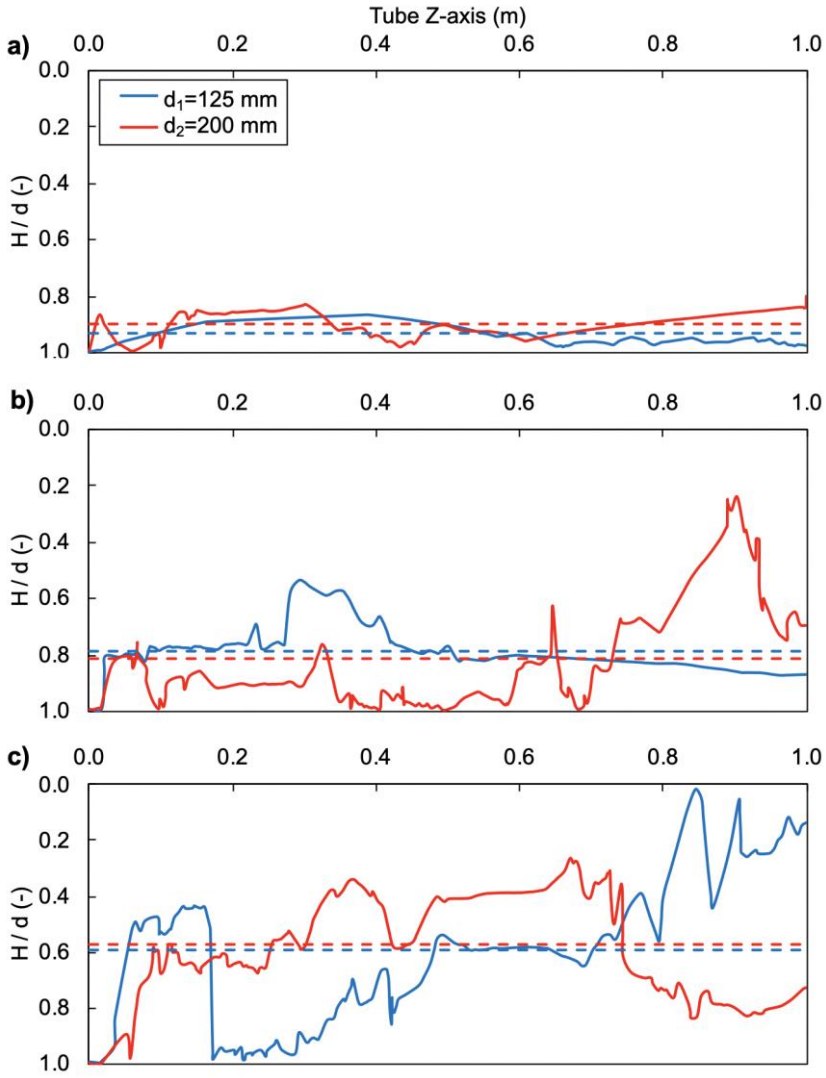

Fig. 4.3.5.2. Dimensionless distance of microalgae cell from the irradiated wall of HHT PBR tube - a) calibration, *Re*=23,700, b) configuration A, *Re*=31,200, c) configuration C, *Re*=46,200. Dashed lines represent the mean values, *H* indicates the distance from the irradiated wall and *d* is the tube diameter.

5 Multi-physical model integrating the hydrodynamics and PBR performance

The aim of this part of the study was to integrate the influence of hydrodynamic conditions into a mechanistic BIO_ALGAE model simulating the cultivation process. For this purpose, a CFD model describing hydrodynamic conditions in a hybrid horizontal tubular photobioreactor was created,

calibrated and validated (chapter 4). By integrating hydrodynamic conditions into a BIO_ALGAE model, it is possible to investigate the influence of operating conditions on the distribution of light in the culture medium and the production of microalgae.

5.1 Model of light attenuation

For the integrated multi-physics cultivation model, the depth of the culture medium in Lambert-Beer's law was replaced by the mean distance of the particle from the irradiated wall H (m), which depends on the hydrodynamic conditions in HHT PBR (Figure 4.3.5.2). Accordingly, the average intensity of light radiation I_{av} (W m^{-2}) acting on microalgal cells in the tube is defined

$$I_{av} = \frac{I_o \cdot \left(1 - e^{(-K_I \cdot X_C \cdot H)}\right)}{K_I \cdot X_C \cdot H} \tag{5.1}$$

where I_o (W m^{-2}) is the incident light intensity, K_I (m^2 g^{-1}) is the extinction coefficient, X_C (g m^{-3}) is the sum of particulate components (microalgae biomass and bacteria). The integrated multi-physics cultivation model also includes the average depth of the culture medium in the retention tanks z_{tank} (m). The average value of z_{tank} is specified based on the level difference on both sides of the tank h_1 and h_2 (Table 4.3.3.1).

5.2 Multi-physics modeling methodology

The overall modeling methodology is shown in Figure 5.2.1. The hydrodynamic CFD model is used to simulate the particle trajectories for which the distance of the particle from the irradiated wall can be generated. Generated data can be subsequently passed to the attenuation model (Eq. 5.1) integrated into BIO_ALGAE model in order to predict the production of microalgal biomass.

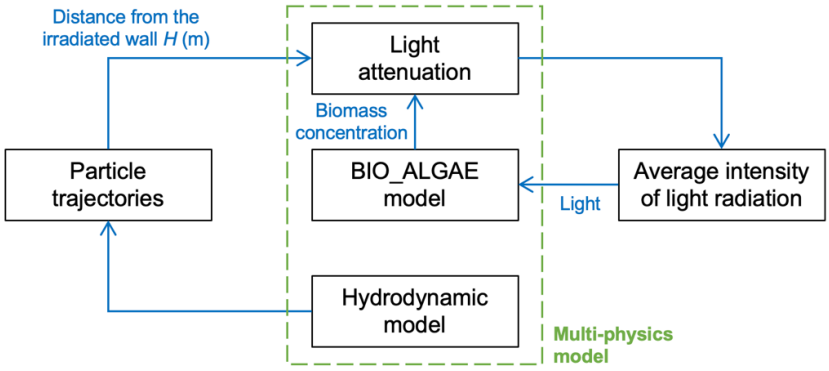

Fig. 5.2.1. Coupling multi-physics methodology of BIO_ALGAE model, hydrodynamics and light attenuation in HHT PBR.

5.3 Model calibration and validation

The model was calibrated using measured data from the winter campaign. The velocity of the culture medium in transparent tubes was set to be 0.25 m s^{-1} during the measuring campaigns, which correspond to configuration A (Table 4.3.3.1). Calibration was performed to minimize the RMSE. The RMSE of the calibrated model for each component was $RMSE_{SO2}$ = 1.36 gO_2 m^{-3}, $RMSE_{TSS}$ = 15.81 gTSS m^{-3} and $RMSE_{NH4}$ = 0.06 gNH_4-N m^{-3}. The model was validated according to experimental data from the spring campaign. Experimental data matched well with simulated data. The

global error of the simulations was slightly higher in comparison with calibration. The RMSE value of each component was $RMSE_{SO2}$ = 2.40 gO_2 m^{-3}, $RMSE_{TSS}$ = 33.24 gTSS m^{-3} and $RMSE_{NH4}$ = 0.10 gNH_4-N m^{-3}.

6 Hydrodynamics influence on microalgae production and light regime

The aim of this chapter was to study the influence of hydrodynamic conditions in HHT PBR on microalgae production. Specifically, this work was carried out to investigate the intensification of the mixing of the culture medium and its subsequent effect on the production of microalgae. Indeed, the CFD hydrodynamic model can simulate the distribution of the microalgae cells in the culture medium during its flow through a transparent tube.

6.1 Hydrodynamics influence on microalgae production

The effect of flow rate on microalgae concentration in culture medium X_{ALG} (g L^{-1}) was not significant based on the value from measuring campaigns. With an increasing flow rate, only a negligible change occurs in X_{ALG} in HHT PBR. The flow regime changes from the *Re*=23,700 to 31,200 leads to 0.21 and 0.12 % increase in X_{ALG} during winter and spring campaigns, respectively. For the flow regime *Re*=46,200, there was an increase of 0.21 % compared to *Re*=23,700 during the spring campaign. A slight increase in X_{ALG} was affected by the generally low production of microalgae. The concentration of microalgae in the culture medium reaching 0.1 g L^{-1} during the winter season and 0.3 g L^{-1} during the spring season. In this case, the culture medium has a low concentration and the light radiation was not limited in the penetration of the culture medium layer. Microalgae production (X_{ALG}) in HHT PBR was limited by a lack of nutrients during both measurement campaigns. More precisely, it was a lack of phosphorus, which was deficient throughout the whole year in influent wastewater. Similar cultivation systems usually reach microalgae concentrations over 1 g L^{-1} (Olivieri et al., 2014). It is possible to adjust the nutrient content of the influent wastewater in order to increase the X_{ALG} reaching the value of 1 g L^{-1}. According to the change of flow regime *Re*=23,700 to 31,200, microalgae production can increase by 0.7 %. Using the created multi-physics model, the cultivation process was simulated for operating conditions that ensure intensive mixing of the culture medium in transparent HHT PBR tubes. Using the validated model, the production of biomass X_{ALG} (g L^{-1}) was simulated under operating conditions that correspond to the flow regime in transparent tubes *Re*=174,700.

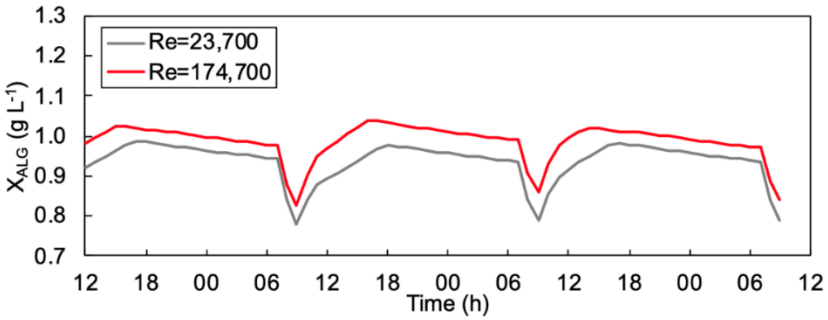

Fig. 6.1.1. Microalgae production for various operating conditions corresponding to flow regime in transparent tubes *Re*=23,700 (shadow line) and *Re*=174,700 (red line).

In Figure 6.1.1, a significant increase in the production of microalgae in comparison with the base flow regime (*Re*=23,700) is shown. For the flow regime in the transparent tube of *Re*=174,700, the biomass production increase by 4.6 % compared to base *Re*=23,700, which results in an increase in biomass production by 99 g day^{-1} from the base 2,145 g day^{-1}.

6.2 Hydrodynamics influence on light regime

Since the transparent HHT PBR tubes were placed on the ground, only the upper part of the tubes could be irradiated. Therefore, if the culture medium in the tube is not sufficiently mixed, the particles located in the lower part of the tube do not receive the required amount of light radiation. The area of the tube where the average light intensity is lower than the critical value of the saturation light intensity is defined as the dark zone. Conversely, in the light zone, the average light intensity is higher. The saturation light intensity for *Chlorella* is reported to range from 67.25 to 96.84 μmol m^{-2} s^{-1} (Cheng et al., 2016; Huang et al., 2014). The critical saturation light intensity for cyanobacteria is lower and reaches values around 50 μmol m^{-2} s^{-1} (Tilzer, 1987). To evaluate the light regime under different operating conditions of HHT PBR, it is possible to use the light fraction ε_L indicating the fraction of the time in the light zone in a light/dark (L/D) cycle. The light fraction is defined by Eq. (6.1)

$$\varepsilon_L = \frac{t_i}{t_L + t_D} \tag{6.1}$$

where t_L (s) is the retention time of microalgae cell in the light zone, and t_D (s) is the time when the cell is in the dark zone. The transition boundary between the light and dark zones can be defined by the critical saturation intensity of the light, which was selected to be 70 μmol m^{-2} s^{-1} (Huang et al., 2014; Tilzer, 1987). The light regime was calculated using Eq. (5.1) for the concentration of microalgae in the culture medium 1 g L^{-1}, and the intensity of incident light corresponding to the spring average daily measured value of 431 W m^{-2}. A tube with a diameter of d_1=125 mm consists of 83 % of a light zone and 17 % of a dark zone. In a tube d_2=200 mm, the total tube volume consists of 55 % of a light zone, and the dark zone reaches 45 %. As the velocity in the tube increases, the particles more often enter the light zone of the tube. Conversely, in the case of the lowest flow velocity (*Re*=23,700), the particles in both tubes do not get out of the dark zone during their entire flow (Figure 4.3.5.2a). For the flow regime *Re*=31,200 (Figure 4.3.5.2b), the light fraction ε_L was 0.128 and 0.075 for the tubes d_1 and d_2, respectively. At a higher velocity of the culture medium, corresponding to the value *Re*=46,200 (Figure 4.3.5.2c), the light fraction in tube d_1 was 0.678, and in tube d_2 was 0.369.

7 Hydrodynamics of flat panel PBR

Simulations of the integrated model showed the positive effect of mixing intensification on increasing microalgal biomass production. It is also possible to use the static mixers in order to intensify the mixing of the culture medium in the irradiated area of the PBR. Another important parameter in scaling-up of the cultivation system is also the formation of a biofilm on transparent walls, which prevents the light irradiation of the culture medium.Hydrodynamics in flat panel photobioreactor (FP PBR) is more complex than in HHT PBR. By comparing the created hydrodynamic model with experimental measurements, the influence of hydrodynamics on the prevention of biofilm formation was specified as well.

7.1 Photobioreactor design and system operation

The volume of the culture medium in the FP PBR chamber is 75 L. The height of the chamber is 2.0 m and the width is 0.7 m. The distance between the transparent plates is 0.05 m. Inlet and outlet ports are located on the chamber and it is possible to change the inflow and outflow of the culture medium from the upper part to the bottom of the FP PBR chamber (Figure 7.1.1). Two necks are located on either side of the lower part of the chamber. One neck is located in the middle of the upper part. The element for the distribution of aeration gas in the culture medium is installed at the bottom of the chamber.

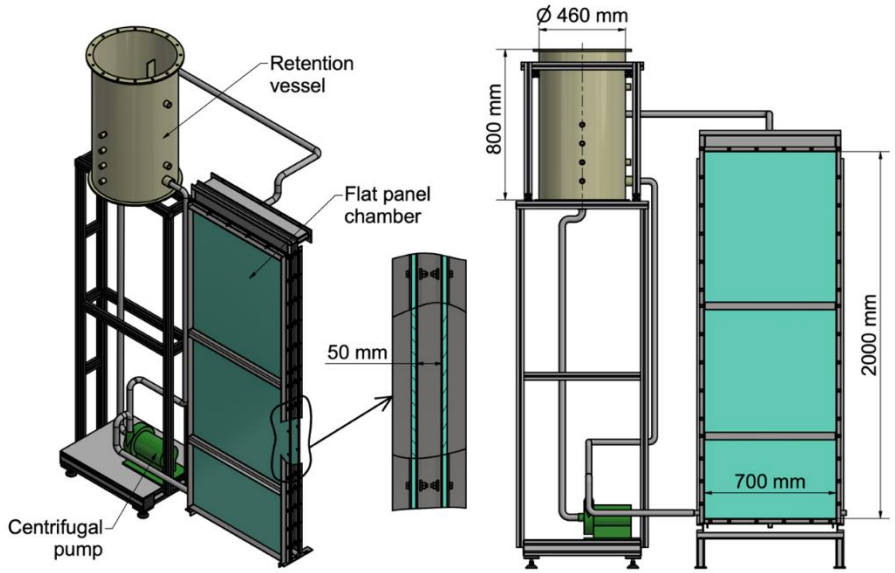

Fig. 7.1.1. 3D drawing of flat panel system.

7.2 Calibration and validation of CFD model

7.2.1 Numerical model setup

Fluid dynamic model setup

The Re-Normalization Group (RNG) k-ϵ model was used to simulate the fluid dynamics behavior in FP PBR. The hydrodynamic conditions were numerically simulated with the software ANSYS FLUENT CFD 19.1.

7.2.2 Model calibration and preliminary validation

The time of homogenization and flow in the FP PBR chamber was measured using a pulse-input tracer method (phenolphthalein reacted with sodium hydroxide). The tracer was applied to the retention vessel and consequently, the streamlines in the FP PBR chamber were visually monitored. At the same time, the homogenization time was measured when the tracer was completely dispersed. The homogenization time was then compared to the hydraulic retention time (HRT) in the FP PBR chamber. The CFD model was created for three setting configurations of the inlet and outlet of the culture medium. The first configuration considers the inflow of the culture medium through the one bottom neck and the outflow through one top neck. In the second configuration, the bottom inlet was divided into two opposite necks. For the third configuration, the valves were set so the inflow of medium is situated through the

top inlet neck and the outflow through the two bottom outlet necks. An experiment with a flow rate of 45 L min^{-1} was created to calibrate the CFD model. Validation of the developed CFD model is needed in order to determine its usability for the simulation of various conditions of FP PBR. In a real FP PBR, the streamlines were monitored for the flow rate of 63 L min^{-1} and subsequently compared to the CFD model. Based on the measurement, it can be determined that the measured and simulated streamlines were in good agreement and the CFD model can be used to simulate various operating conditions in FP PBR.

7.3 Hydrodynamic conditions in FP PBR

7.3.1 Velocity distribution and flow regime

The configuration with one bottom inlet (Figure 7.3.1.1a) reaches the highest flow velocities in the chamber. However, the flow in the chamber forms a circulation loop, which can result in the formation of dead zones in the central part of the chamber. In the case of the configuration with a double bottom inlet (Figure 7.3.1.1b), the flow rate was still high. The inflows of the culture medium were directed against each other, which results in a mutual dispersion of the flow, which ensures a more uniform flow in the central part of the FP PBR chamber. In the case of the top inlet configuration (Figure 7.3.1.1c), the culture medium in the chamber reaches the lowest velocities. However, the flow was the most uniform in the central part of the chamber.

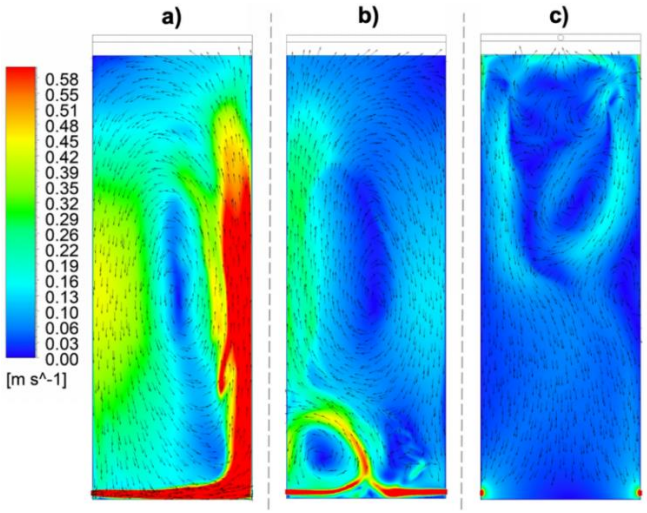

Fig. 7.3.1.1. Velocity distribution in FP PBR chamber – flow rate: 63 L min^{-1}. a) single bottom inlet and top outlet, b) double bottom inlet and top outlet, c) top inlet and double bottom outlet.

The time when the tracer was completely dispersed was also determined for each configuration. From a comparison of the homogenization time and the HRT (Table 7.3.1.1), it was evident that the homogenization time was significantly higher for the top inlet configuration than in the case of both bottom inlet configurations. Therefore, low intensity mixing occurs during the top inlet configuration. The single bottom inlet configuration achieves the highest velocities in the chamber; however, the homogenization time was comparable to HRT at a flow rate of 45 L min^{-1}, and even higher at a flow rate

of 63 L min^{-1}. In the configuration with a double bottom inlet, the most intensive mixing occurs, since the homogenization time was lower than the HRT for both flow rates.

Table 7.3.1.1. Homogenization time and HRT in FP PBR chamber.

Inflow (L min^{-1})	Homogenization time (s)			HRT (s)
	Top inlet	Single bottom inlet	Double bottom inlet	
45	143	97	78	97
63	126	75	64	69

7.3.2 Biofilm formation

Biofilm removal has an important role in closed cultivation systems. Biofilm is visible as a thin viscous layer of sediments, and its thickness can reach hundreds of micrometers. Biofilm formation reduces light intensity entering into the system (Zippel and Neu, 2005). The effect of shear force on the wall, respectively, the wall shear stress τ_w (Pa s) can disrupt the stability of the microalgae biofilm.

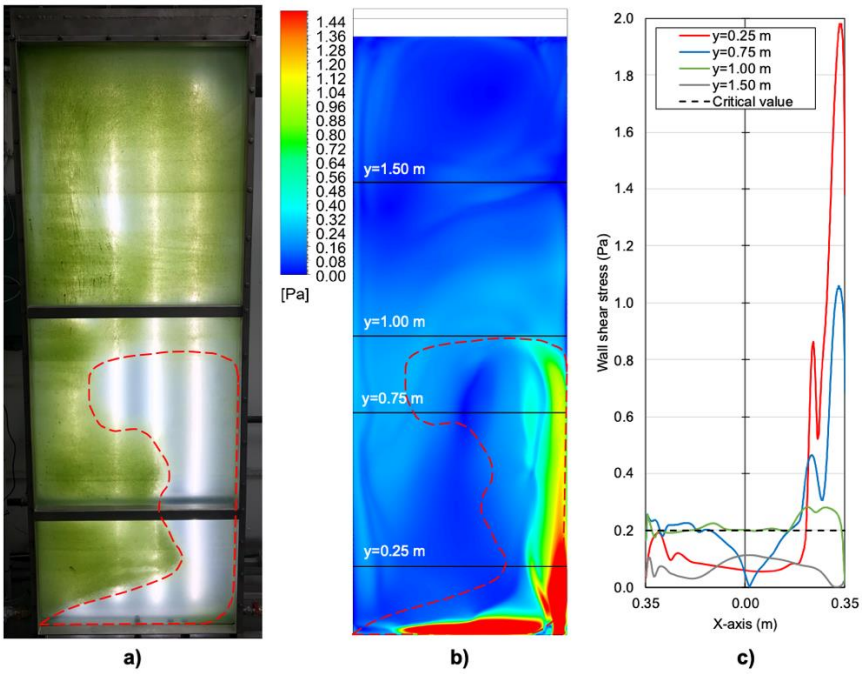

Fig. 7.3.2.1. Comparison of experimental microalgae biofilm formation and CFD simulation of wall shear stress distribution in FP PBR chamber, flow rate: 45 L min^{-1} – a) fixed biofilm on transparent plate, b) wall shear stress distribution, c) distribution of wall shear stress along the selected cross-sections.

Therefore, it is important to define the critical value of the wall shear stress, which can prevent the formation of biofilm. The biofilm fixed on a transparent plate of FP PBR at a flow rate of 45 L min^{-1} is shown in Figure 7.3.2.1a. Microalgae formed a thin layer of biofilm on the transparent plates, which prevent the irradiation of the culture medium. However, the biofilm formation does not occur in locations with high flow velocities. A simulation of wall shear stress distribution on the transparent plates was developed for the same flow rate (Figure 7.3.2.1b). The distribution of wall shear stress along the horizontal X-axis is shown in Figure 7.3.2.1c. According to the comparison of wall shear stress

distribution on the transparent walls and the formed biofilm, it is possible to determine the critical wall shear stress value. At wall shear stress values τ_w higher than 0.2 Pa, the biofilm formation does not occur. From the wall shear stress distribution in Figure 7.3.2.1b, the area with wall shear stress below critical value accounts for 70 % of the total FP PBR transparent plate area.

7.3.3 Wall shear stress

Using the validated CFD model for the single bottom inlet configuration, the wall shear stress distribution was also created for the culture medium flow rate of 63 L min^{-1}. By increasing the flow rate to 63 L min^{-1}, the area with wall shear stress below critical value avoiding formation of biofilm was reduced to 33 %. However, at the top of the PBR chamber, the wall shear stress was still below the critical value. Also, the circulating loop begins to form in the central part of the chamber. This loop causes non-intensive mixing of culture medium at the center of the FP PBR chamber and wall shear stress on the wall was low as well. Therefore, another operating or design settings of the cultivation system need to be applied in order to eliminate this area.

8 Homogenization and mixing of flow in flat panel PBR

The aim of this work was to design a static mixer that could be installed in the FP PBR chamber. The static mixer should ensure the distribution of the medium flow throughout the cross-section of the chamber, ensure homogenous residence time of the culture medium in the irradiated area, and further intensify the mixing of the culture medium.

8.1 Static mixer

The design of the static mixer was inspired by the geometry of conventional Sulzer SMX and SMV static mixers, which can be installed in tubes of circular cross-section. The geometry and application of the static mixer is protected as a utility model (U1 34 865 CZ, registered Feb 23, 2021) and an application for a European patent was submitted as well. The static mixer was located at a distance of 0.46 m from the bottom inlets (Figure 8.1.1).

Fig. 8.1.1. Static mixer in FP PBR chamber.

8.2 Calibration and validation of CFD model

8.2.1 Numerical model setup

The geometry of the chamber with the static mixer mostly corresponds to the model for the empty chamber. The geometry and mesh were created in the ANSYS system. In the part of the static mixer, the mesh was refined in order to simulate the flow in this area.

8.2.2 Model calibration and preliminary validation

A model for a flow rate of 45 L min^{-1} was created to calibrate the CFD model. Validation of the developed CFD model is needed in order to determine its usability for the simulation of various conditions of FP PBR with the static mixer. The streamlines were monitored for the flow rate of 63 L min^{-1} and subsequently compared to the CFD model. Based on the measurement, it can be determined that the measured and simulated streamlines were in good agreement and the CFD model can be used to simulate various operating conditions in FP PBR with an installed static mixer.

8.3 Hydrodynamic conditions in FP PBR with static mixer

8.3.1 Velocity distribution and flow regime

The single bottom inlet configuration (Figure 8.3.1.1) creates a circulation loop in the lower part of the chamber below the static mixer, which prevents the medium from flowing homogeneously through the segments of the static mixer. Due to the inflow located on one side of the static mixer, a circulation loop was formed in the upper part of the FP PBR chamber as well as in the bottom part. The double bottom inlet configuration ensures a more uniform flow of medium to the center of the static mixer. By installing another static mixer with the inverted rotation of the blades, it would be possible to eliminate the flow on the side of the chamber and further intensify the process of mixing the culture medium.

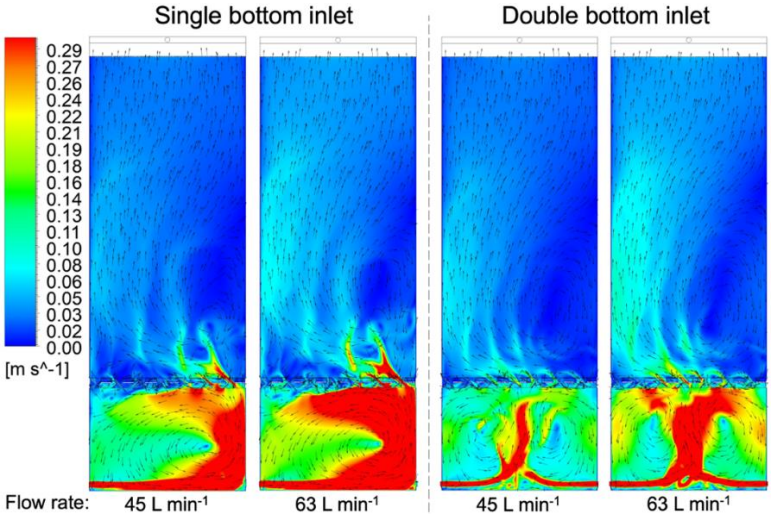

Fig. 8.3.1.1. Velocity distribution in FP PBR chamber with static mixer.

The time when the tracer was completely dispersed was also determined. Table 8.3.1.1 and Table 8.3.1.2 show the homogenization times and the HRT for each culture medium flow rate and for the configurations with and without the static mixer.

Table 8.3.1.1. Single bottom inlet configuration - comparison of homogenization time and HRT in empty FP PBR chamber and FP PBR chamber with static mixer.

Inflow (L min^{-1})	HRT (s)	FP PBR chamber	Homogenization time (s)
45	97	Empty	97
		Static mixer	113
63	69	Empty	75
		Static mixer	78

For the double bottom inlet configuration, there was a significant change when comparing an empty chamber and a chamber with a static mixer. Using the static mixer, the homogenization time was reduced by 13 s and 22 s at a flow rate of 45 L min^{-1} and 63 L min^{-1}, respectively.

Table 8.3.1.2. Double bottom inlet configuration - comparison of homogenization time and HRT in empty FP PBR chamber and FP PBR chamber with static mixer.

Inflow (L min^{-1})	HRT (s)	FP PBR chamber	Homogenization time (s)
45	97	Empty	78
		Static mixer	65
63	69	Empty	64
		Static mixer	42

8.3.2 Wall shear stress

The configuration of FP PBR with a static mixer is more suitable from the point of view of uniformity of HRT of the processed culture medium in the irradiated area of the FP PBR. However, on the contrary from the point of view of the effect of the wall shear forces on the stability of the formed biofilm seems to be a more suitable configuration with an empty chamber.

8.3.3 Pressure drop

The pressure drop *Δp* (Pa) in the FP PBR chamber was measured for different flow rates of the culture medium. The difference between the pressure drop in the empty chamber and the pressure drop in the chamber with the static mixer shows that at a flow rate of 45 L min^{-1} the pressure drop of the static mixer reaches 0.9 kPa and at a flow rate of 63 L min^{-1} the pressure drop was 1 kPa. At a flow rate of 45 L min^{-1}, the analytically calculated pressure drop in the empty chamber of the FP PBR is 1.71 kPa and at a flow rate of 63 L min^{-1} the pressure drop is 3.35 kPa. The dimensionless friction coefficient of the static mixer λ_s can be derived from Darcy-Weissbach equation. Since the measurements were made for only one geometry of the FP PBR chamber, it is convenient to use a more general notation, i.e. the dependence of $\lambda_s(L_s/d_h)$ on *Re* (Figure 8.3.3.1).

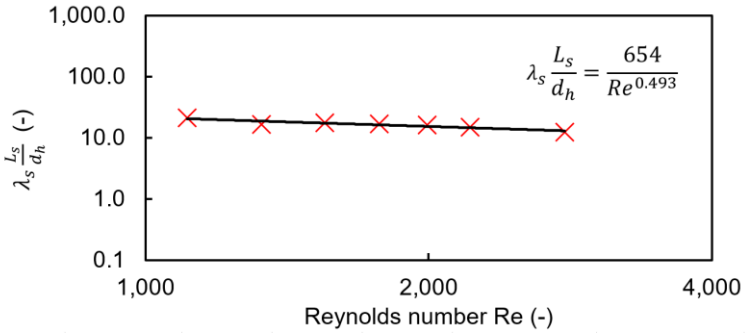

Fig. 8.3.3.1. Experimental dependence of friction coefficient on Reynolds number for the developed static mixer installed in the FP PBR chamber.

It is evident that in the region of the lower turbulent *Re*, the dimensionless friction coefficient λ_s slightly decreases with increasing *Re*. Conventional tubular static mixers demonstrate a similar behavior at operating conditions approaching the critical *Re* defining the transition between laminar and turbulent flow regime (Kabátek et al., 1989; Li et al., 1997).

8.3.4 Set of static mixers

In order to eliminate this imbalance and at the same time intensify the mixing of the medium in the chamber, another static mixer was created in the model at a distance of 200 mm. The second static mixer has the angle of inclination of the blades perpendicular to the transparent walls opposite to the first static mixer. Using the created numerical model of two static mixers in the FP PBR chamber, a simulation of the medium flow velocity distribution was created (Figure 8.3.4.1).

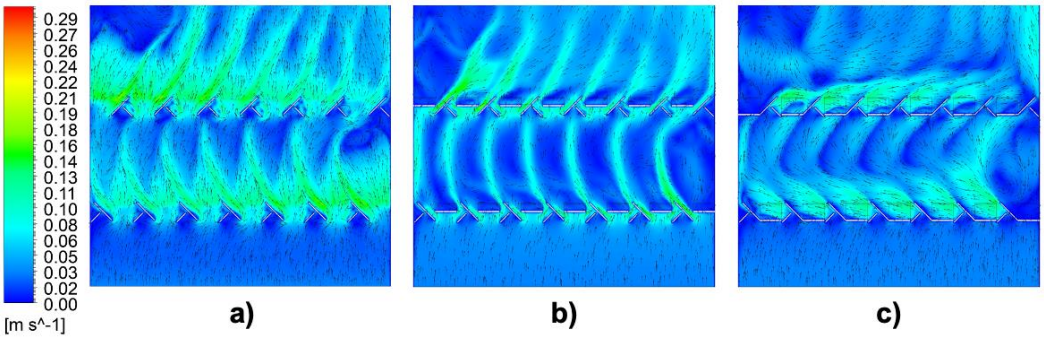

Fig. 8.3.4.1. Velocity distribution in FP PBR chamber with two static mixers – detail view, flow rate: 63 L min^{-1} – a) front wall, b) middle plane, c) back wall.

The highest values of the flow velocity were reached near the front wall (Figure 8.3.4.1a). On the back wall (Figure 8.3.4.1c), the flow was directed towards the side of the FP PBR chamber since the flow was influenced essentially only by the blades, which are perpendicular to the transparent walls. Due to the opposite blade's inclination, the medium was more evenly distributed over the entire width of the chamber.

9 Conclusions

The following conclusions can be drawn from the results obtained in this thesis.

- Based on intensive experimental measurements of HHT PBR performance, the mechanistic BIO_ALGAE model was calibrated and validated. The BIO_ALGAE can simulate the production of microalgae; however, the model does not consider the influence of hydrodynamic conditions and works with the assumption that the culture medium is perfectly mixed. Experimental measurements of hydrodynamic conditions were performed on the same HHT PBR. Based on the results of hydrodynamic measurements, the CFD model hydrodynamic conditions were calibrated and validated. By increasing the flow rate of the culture medium, it was not possible to completely eliminate the formation of dead zones in open tanks. The intensification of mixing in the HHT PBR tubes due to the increasing flow rate (*Re*=23,700 to *Re*=46,200) results in an increase in shear stress on the transparent walls (0.3 Pa to 1 Pa). The wall shear forces are important in terms of elimination of biofilm formation, where the critical value avoiding the formation reaches 0.2 Pa. The movement of microalgal cells in transparent tubes was also simulated for different flow rates. Intensification of mixing (*Re*=23,700 to *Re*=46,200) results in a more frequent transition of cells between the dark and light zones (the light fraction increased to 0.678), which has a significant effect on production.

- The particle trajectory was subsequently integrated into a multi-physical model, which combines a mechanistic BIO_ALGAE model and a hydrodynamic CFD model. Using the created multi-physical model, it is possible to predict the influence of hydrodynamic conditions on the light attenuation in the culture medium and the subsequent microalgae production. The created multi-physical model showed an increase in the concentration of microalgae by 2 % due to the mixing intensification (*Re*=23,700 to *Re*=46,200). Increasing the flow rate to the maximum value (*Re*=174,700) may increase the concentration by 4.6 %. However, further intensification of mixing is limited by the operating and design parameters of HHT PBR and it would be necessary to optimize the system design by installing static mixers in transparent tubes.
- The hydrodynamic CFD model of FP PBR was calibrated and validated based on the experimental measurements. Hydrodynamic conditions in the FP PBR chamber were studied for different flow rates (45 and 63 L min^{-1}) and different configurations of inlet and outlet settings (top inlet, single bottom inlet, double bottom inlets). The most intensive mixing and homogenization of the culture medium in the FP PBR chamber occur in a double bottom inlet configuration, as the homogenization time (78 and 64 s for 45 and 63 L min^{-1} inflow) is lower than HRT (97 and 69 s). From the point of view of preventing the formation of biofilm on the transparent wall of FP PBR, a configuration with a single bottom inlet appears to be the most suitable. At a flow rate of 45 L min^{-1}, the wall shear stress on 70 % of the transparent wall of the FP PBR reaches a value lower than the critical value of the shear stress preventing the formation of biofilm (0.2 Pa). At a flow rate of 63 L min^{-1}, the area is reduced to 33 %. However, by increasing the flow rate, the formation of dead zones in any inlet configuration cannot be prevented, and the flow of the culture medium needs to be more homogenized throughout the cross section of the FP PBR chamber.
- A static mixer was designed in order to intensify the mixing and homogenize the flow in the FP PBR chamber. For a single bottom inlet configuration, the installation of a static mixer did not shorten the homogenization time for any of the selected flow rates. However, in the double bottom inlet configuration, the homogenization time was reduced by 17 % at a flow rate of 45 L min^{-1} and 34 % at a flow rate of 63 L min^{-1}. The flow of the culture medium was homogeneous in almost the entire cross-section of the FP PBR chamber. By installing series-connected static mixers (vertical distance 200 mm) it was possible to eliminate the formation of dead zones in the FP PBR chamber.

10 References

Belohlav, V., Jirout, T., 2019. Design methodology of industrial equipment for microalgae biomass primary harvesting and dewatering. Chem. Eng. Trans. 76, 919–924. https://doi.org/10.3303/CET1976154

Belohlav, V., Zakova, T., Jirout, T., Kratky, L., 2020. Effect of hydrodynamics on the formation and removal of microalgal biofilm in photobioreactors. Biosyst. Eng. 200, 315–327. https://doi.org/10.1016/j.biosystemseng.2020.10.014

Cheng, W., Huang, J., Chen, J., 2016. Computational fluid dynamics simulation of mixing characteristics and light regime in tubular photobioreactors with novel static mixers. J. Chem. Technol. Biotechnol. 91, 327–335. https://doi.org/10.1002/jctb.4560

Chisti, Y., 2016. Large-Scale Production of Algal Biomass: Raceway Ponds, in: Algae Biotechnology. Springer, Cham, pp. 21–40. https://doi.org/10.1007/978-3-319-12334-9_2

Huang, J., Li, Y., Wan, M., Yan, Y., Feng, F., Qu, X., Wang, J., Shen, G., Li, W., Fan, J., Wang, W., 2014. Novel flat-plate photobioreactors for microalgae cultivation with special mixers to promote mixing along the light gradient. Bioresour. Technol. 159, 8–16. https://doi.org/10.1016/j.biortech.2014.01.134

Kabátek, J., Ditl, P., Novák, V., 1989. Helax-a new type of static mixer-operation characteristics and comparison with other types. Chem. Eng. Process. 25, 59–64. https://doi.org/10.1016/0255-2701(89)80031-5

Li, H.Z., Fasol, C., Choplin, L., 1997. Pressure drop of newtonian and non-newtonian fluids across a sulzer SMX static mixer. Chem. Eng. Res. Des. 75, 792–796. https://doi.org/10.1205/026387697524461

Masojídek, J., 2014. Mass Cultivation of Freshwater Microalgae. Earth Syst. Environ. Sci. 1–13. https://doi.org/10.1016/B978-0-12-409548-9.09373-8

Milano, J., Ong, H.C., Masjuki, H.H., Chong, W.T., Lam, M.K., Loh, P.K., Vellayan, V., 2016. Microalgae biofuels as an alternative to fossil fuel for power generation. Renew. Sustain. Energy Rev. 58, 180–197. https://doi.org/10.1016/j.rser.2015.12.150

Olivieri, G., Salatino, P., Marzocchella, A., 2014. Advances in photobioreactors for intensive microalgal production: Configurations, operating strategies and applications. J. Chem. Technol. Biotechnol. 89, 178–195. https://doi.org/10.1002/jctb.4218

Perner-Nochta, I., Posten, C., 2007. Simulations of light intensity variation in photobioreactors. J. Biotechnol. 131, 276–285. https://doi.org/10.1016/j.jbiotec.2007.05.024

Solimeno, A., Acíen, F.G., García, J., 2017. Mechanistic model for design, analysis, operation and control of microalgae cultures: Calibration and application to tubular photobioreactors. Algal Res. 21, 236–246. https://doi.org/10.1016/j.algal.2016.11.023

Tilzer, M.M., 1987. Light-dependence of photosynthesis and growth in cyanobacteria: Implications for their dominance in eutrophic lakes. New Zeal. J. Mar. Freshw. Res. 21, 401–412. https://doi.org/10.1080/00288330.1987.9516236

Zakova, T., Jirout, T., Kratky, L., Belohlav, V., 2019. Hydrodynamics as a tool to remove biofilm in tubular photobioreactor. Chem. Eng. Trans. 76, 451–456. https://doi.org/10.3303/CET1976076

Zhang, Q., Wu, X., Xue, S., Liang, K., Cong, W., 2013. Study of hydrodynamic characteristics in tubular photobioreactors. Bioprocess Biosyst. Eng. 36, 143–150. https://doi.org/10.1007/s00449-012-0769-2

Zippel, B., Neu, T.R., 2005. Growth and structure of phototrophic biofilms under controlled light conditions. Water Sci. Technol. 52, 203–209. https://doi.org/10.2166/wst.2005.0202

11 Publications of the author

Articles in refereed journals

Belohlav, V., Uggetti, E., García, J., Jirout, T., Kratky, L., Díez-Montero, R. (2021) Assessment of hydrodynamics based on Computational Fluid Dynamics to optimize the operation of hybrid tubular photobioreactors, *Journal of Environmental Chemical Engineering*, 9, 105768.

Belohlav, V., Jirout, T., Kratky, L. (2021) Optimization of hydrodynamics by installation of static mixer in flat panel photobioreactor. *Chemical Engineering Transactions*, 86.

Belohlav, V., Zakova, T., Jirout, T., Kratky, L. (2020). Effect of hydrodynamics on the formation and removal of microalgal biofilm in photobioreactors. *Biosystems Engineering*, 200, 315–327.

Díez-Montero, R., Belohlav, V., Ortiz, A., Uggetti, E., García-Galán, M. J., García, J. (2020). Evaluation of daily and seasonal variations in a semi-closed photobioreactor for microalgae-based bioremediation of agricultural runoff at full-scale. *Algal Research*, 47, 101859.

Belohlav, V., Jirout, T. (2019). Design methodology of industrial equipment for microalgae biomass primary harvesting and dewatering. *Chemical Engineering Transactions*, 76, 919–924.

Belohlav, V., Jirout, T., Kratky, L. (2018). Possibilities of implementation of photobioreactors on industrial scale. *Chemické Listy*, 112 (3), 183–190.

García, J., Ortiz, A., Álvarez, E., Belohlav, V., García-Galán, M. J., Díez-Montero, R., Álvarez, J. A., Uggetti, E. (2018). Nutrient removal from agricultural run-off in demonstrative full scale tubular photobioreactors for microalgae growth. *Ecological Engineering*, 120.

Zakova, T., Jirout, T., Kratky, L., Belohlav, V. (2018). Hydrodynamics as a tool to remove biofilm in tubular photobioreactor. *Chemical Engineering Transactions*, 76, 451–456.

Belohlav, V., Jirout, T., Kratky, L., Uggetti, E., Díez-Montero, R., García, J. (in preparation). Integration of hydrodynamics in cultivation model of hybrid horizontal tubular photobioreactor.

Belohlav, V., Jirout, T., Kratky, L., Uggetti, E., Díez-Montero, R., García, J. (in preparation). Mutual hydrodynamics and light regime influence on microalgae biomass production in a hybrid horizontal tubular photobioreactor.

Conference proceedings

Belohlav, V., Jirout, T., Kratky, L. (2017). Operational and design parameters of microalgae cultivation systems for its application in industrial scale. In European Biomass Conference and Exhibition Proceedings; ETA – Florence, pp 1990–1997.

Belohlav, V., Uggetti, E., Montero, R. D., García, J., Jirout, T., Kratky, L. (2018). Numerical investigation of hydrodynamic conditions in a pilot tubular photobioreactor. In European Biomass Conference and Exhibition Proceedings; ETA – Florence, pp 183–190.

Belohlav, V., Jirout, T. (2019). Equipment for microalgae primary dewatering and separation using gravitational and centrifugal forces. In European Biomass Conference and Exhibition Proceedings; ETA – Florence, pp 1957–1962.

Belohlav, V., Jirout, T., Kratky, L., Uggetti, E., Díez-Montero, R. (2019). Numerical analysis of hydrodynamic conditions in pilot flat-panel photobioreactor: operating and design parameters influence on the microalgae cultivation. In European Biomass Conference and Exhibition Proceedings; ETA - Florence, pp 255–260.

Belohlav, V., Jirout, T., Kratky, L. (2021). Integration of hydrodynamics into a biokinetic model for the simulation of microalgae cultivation in a photobioreactor. In European Biomass Conference and Exhibition Proceedings; ETA – Florence, Proceedings Pre-proof.

Utility model

Jirout, T., Belohlav, V. Static mixer, especially into a plate reactor chamber, U1 34 865 CZ, Feb 23, 2021.

European patent

Jirout, T., Belohlav, V. Static mixer, especially into a plate reactor chamber (submitted).